A Statistical Cell Delay Model for Estimating the 3σ Delay by Matching Kurtosis

Leilei Jin, Wenjie Fu, Hao Yan, and Longxing Shi, *Member, IEEE*

***Abstract*—Accurate standard cell modeling is significant for circuit timing analysis and yield estimation. With voltage decreasing to near-threshold, cell delay distribution becomes asymmetrical and has a longer tail due to various process variation effects. In this brief, we propose a novel statistical model to fit the shape of the cell delay by using log-extended-skew-normal (LESN) distribution. It estimates the values of mean, standard deviation, and 3σ delay precisely by matching the kurtosis of the cell delay distribution. By changing the parameters of the LESN model, it can be used for up to the normal voltage region (1.1V) and down to the sub-threshold voltage region (0.4V). Considering the effect of load capacitances, the parameters of LESN distribution are further modeled so that the model can be used for different fanout constraints. Tested by INV, NAND2, and NOR2 with 28 nm technology, the average error of estimating the skewness is less than 6%, while the error for the kurtosis is less than 4%. Meanwhile, the average errors of -3σ and $+3\sigma$ delay estimation are about 1.27% and 1.82% from 0.4V to 1.1V, respectively.**

***Index Terms*—Delay distribution, process variations, standard cell models, sub-threshold voltage.**

I. Introduction

TIMING analysis is one of the main procedures in the circuit design flow. It not only provides the basis for physical design optimizations but also provides the worst-case circuit delay for the timing sign-off. In advanced technology nodes, the impact of process variation is increasing, leading to unpredictable circuit delays. Although device-level simulators can capture golden results in the form of probability distributions through Monte Carlo sampling, the simulation is always impractically slow. Deterministic static timing analysis can be used to quickly analyze large circuits. It spreads the delay of each cell by reading a pre-build cell delay library file, which stores the cell delays of each corner based on the look-up table (LUT) approach. When recording the impacts of process variations, the number of LUTs increases, bringing unacceptable analysis and storage overhead. To model the statistical behavior efficiently, statistical static timing analysis (SSTA) is proposed to quantify the probability density function (PDF) of the path delay distribution [1]. The distribution is analyzed through the delay of each cell, which is modeled as PDF by introducing Gaussian random variables instead of using LUTs.

Cell delay models can be divided into two categories: using analytical expressions and using empirical models. Analytical approaches provide relationships between cell delays and drain currents. The detailed drain current model is studied considering process variations and the load capacitance of the cell [2]. When the supply voltage is scaled down to near-threshold and sub-threshold, it's hard to build an accurate delay model because of the complicated effect of process variations. Therefore, recent proposed analytical expressions are studied based on simplified scenarios, for example, only taking the threshold voltage variation into consideration [3], [4]. Empirical models treat the cell as a black box, and construct the relationship between inputs and outputs by means of fittings or regressions. Data for building the model is based on Monte Carlo simulations. Regression-based methods construct the relationship between cell delay and process variations [5] while fitting-based methods directly fit the shape of its PDF and usually show higher accuracies [6].

In fitting-based methods, the cell delay distribution is considered to be a Gaussian distribution at normal supply voltage and can be accurately estimated using a first-order canonical model [7] or higher-order forms [5]. When the voltage is scaled down, the process variation effect on the cell delay is not linear, which leads the distribution to be non-Gaussian. Several researches propose cell delay models based on other distribution forms, such as Burr distribution [8], skew-normal distribution [9], and log-skew-normal distribution [6]. These models can get results with higher accuracies based on a specific process variation impact, e.g., V_{th}, X_L. But in the SPICE MOSFET model from the foundry, various process variations affect the cell delay simultaneously. The distribution turns more asymmetric and its right tail turns longer and fatter. It causes low-probability events more likely to occur when the supply voltage drops down to near-/sub-threshold regions. However, previous studies mainly focus on the skewness modeling of the distribution to quantify the asymmetry [6], [9]. As the tail shape is not well modeled, these models lead to large errors in estimating the $+3\sigma$ delay of the delay distribution, as well as the -3σ delay, which is bad for the worst-case analysis of hard real-time system design [10], [11].

To cover the tail shape and asymmetry of the delay distribution, we propose a novel statistical cell delay model using

Manuscript received November 11, 2021; revised February 3, 2022; accepted March 1, 2022. Date of publication March 9, 2022; date of current version May 27, 2022. This work was supported in part by the National Key Research and Development Program of China under Grant 2018YFB2202702, and in part by the National Natural Science Foundation of China under Grant 61874152. This brief was recommended by Associate Editor X. Li. *(Corresponding author: Longxing Shi.)*

The authors are with the Technology of National ASIC System Engineering Research Center, Southeast University, Nanjing 210096, China (e-mail: leileijin@seu.edu.cn; lxshi@seu.edu.cn).

Color versions of one or more figures in this article are available at https://doi.org/10.1109/TCSII.2022.3157981.

Digital Object Identifier 10.1109/TCSII.2022.3157981

1549-7747 © 2022 IEEE. Personal use is permitted, but republication/redistribution requires IEEE permission.
See https://www.ieee.org/publications/rights/index.html for more information.

Authorized licensed use limited to: Chinese University of Hong Kong. Downloaded on November 22,2026 at 12:59:40 UTC from IEEE Xplore. Restrictions apply.

the log-extended-skew-normal (LESN) distribution. The LESN distribution can set four parameters to match the mean, standard deviation, skewness and long-tail shape concurrently. By modifying the parameters of the LESN model, it can reduce to a log-skew-normal distribution for simplified process variation scenarios and reduce to a log-normal distribution for higher supply voltage regions. Furthermore, the effect of load capacitance is also quantified. The four parameters of the LESN model can be calculated by linear fittings when the load capacitance is changed. Hence, the cell delay model is suitable for different fanout constraints (e.g., FO1, FO4).

The rest of this brief is constructed as follows: Section II presents related works on statistical cell delay models. Section III introduces characteristics of the delay distribution. The modeling details are discussed in Section IV and the modeling accuracy is given in Section V. Finally, Section VI concludes this brief.

II. Related Works

The first-order canonical cell model is the first proposed regression-based method to model the delay distribution by assuming a linear relationship between process variations and cell delays [7]. When the technology node and supply voltage are scaled-down, the non-linear process variation effect turns the delay distribution to be non-Gaussian. Quadratic and higher-order Taylor functions of process variations are proposed for the non-linearity subsequently [5], [12]. By replacing the second-order items by an Skew-normal (SN) random variable, the model error and computation complexity can be further decreased [13]. Apart from Taylor-based regression models, reference [14] uses multivariate adaptive regression splines (MARS) to effectively model the relationship between process variations and cell delays, without assuming a predetermined form. In [15] and [16], the MARS-based model is further studied for wide voltage SSTA and micro-architecture evaluation.

On the other hand, fitting-based models directly estimate the PDF of delay distribution by introducing a Gaussian random variable. To model the asymmetry of the distribution, [9] adds a parameter to shift the Gaussian density function to the left side to match the actual delay distribution. As the threshold voltage exponentially affects the delay distribution, the log-skew-normal (LSN) based models are proposed that take the logarithm of the delay and then fit it to an SN density function [4], [6]. They have higher accuracies on estimating the mean, standard deviation, and skewness of the delay distribution. However, these regression-based and fitting-based models focus on the asymmetry of the distribution rather than the long tail feature, which leads to large errors in estimating the $+/-3\sigma$ delay of the distribution.

III. Characteristics of Delay Distribution

The characteristics of distribution have two aspects: moments that determine the shape and yields that reflect the best and worst delay. The first-order moment of the distribution is the mean value and the second-order moment is the square of its standard deviation. The third-order moment can be used to quantify the asymmetric of delay distribution under low voltages, which is called skewness [6]. It equals to 0 in symmetrical distribution and becomes larger when the distribution shifts to the left.

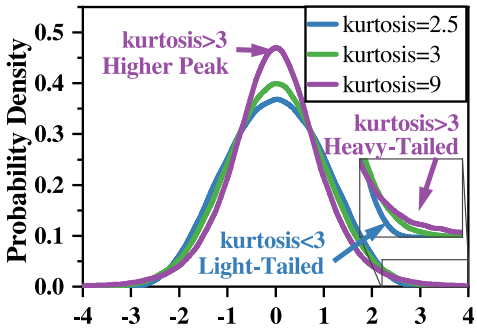

Fig. 1. The effect of Kurtosis on the characteristic of the tail.

Apart from the asymmetry, the tail of the distribution at near-threshold and sub-threshold regions becomes heavier and causes low-probability events more likely to occur. The fourth-order moment, kurtosis, is a statistical measure that defines how heavily the tail of the distribution differs from the tail of a Gaussian distribution [21]. Given random samples X, the kurtosis of the distribution can be calculated by the expectation of $(X-\mu)^4$ divided by σ^4, shown in (1). μ and σ are the mean and standard deviation, respectively. Fig. 1 gives the PDFs with different values of kurtosis. In the Gaussian distribution, the kurtosis is a fixed value of 3. When the kurtosis is increased, the distribution is heavy-tailed (fatter tail) and shows a higher peak. On the contrary, the peak becomes lower and the distribution is light-tailed (thinner tail).

$$\text{kurtosis} = \frac{E\left[(X-\mu)^4\right]}{\sigma^4} \tag{1}$$

For MOSFET devices in SMIC 28 nm, there are more than twenty process variations. To avoid unnecessary details of computations, previous works assume that V_{th} and X_L are two main process variations that affect the cell delay and they build the delay models without setting other process variations [6], [8], [18]–[20]. However, these ignored process variations significantly affect the kurtosis, which leads to a higher probability at the tail of the distribution. Fig. 2 shows the comparisons of the first four moments with different simplifications: only setting X_L, only setting V_{th}, setting both X_L and V_{th}, and setting all process variations. In the near-threshold region, these ignored process variations make the second and third-order moments of the delay distribution increase two times while making the kurtosis increase more than 8 times.

To ensure the high yield of a low voltage design, two values of the delay distribution need to be quantified, which are the -3σ delay (0.14%) for the best-case analysis and $+3\sigma$ delay (99.86%) for the worst-case analysis. In the Gaussian distribution, the $+/-3\sigma$ can be directly calculated by the mean value plus/minus three times the standard deviation. At low voltages, the skewness causes the delay distribution left-offset, which leads to a lower probability near the end of the right tail. However, as the kurtosis increases significantly, the

Authorized licensed use limited to: Chinese University of Hong Kong. Downloaded on November 22,2026 at 12:59:40 UTC from IEEE Xplore. Restrictions apply.

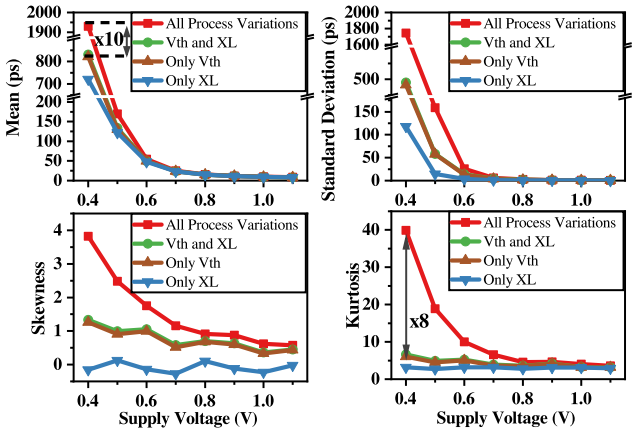

Fig. 2. First four moments under different simplifications of process variations, from 0.4V to 1.1V (SMIC 28 nm, INVX1).

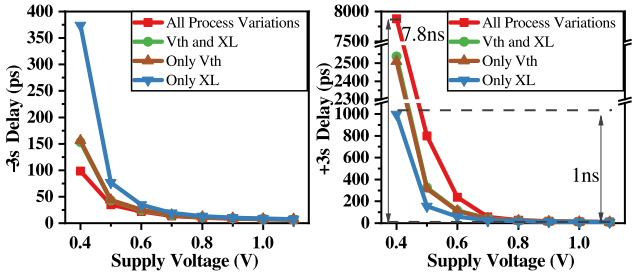

Fig. 3. $+/-3\sigma$ delay under different simplifications of process variations, from 0.4V to 1.1V (SMIC 28 nm, INVX1).

probability near the end of the right tail will be higher than the probability of a distribution modeled only by matching skewness. This is the reason why traditional cell delay models have a large skewness to quantify the degree of left-shift of the distribution, but $+3\sigma$ delay increases inversely. Fig. 3 shows the impact of different process variation simplifications on $+/-3\sigma$ delay estimations. In the simplified scenarios, kurtosis is increased slightly so that the $+3\sigma$ remains almost a constant. After considering all process variations, the kurtosis increases 8 times, and the $+3\sigma$ delay increases.

IV. Delay Modeling Using Log-Extended-Skew-Normal Distribution

A. Extended-Skew-Normal Distribution

Skew-normal (SN) is well studied on delay distribution modeling, but fails to match the first four moments due to the SN distribution merely having three parameters. Extended-skew-normal (ESN) distribution is an extension of SN distribution, which needs four parameters to determine the shape of the distribution [17]. The density function of a standard ESN random variable is given in (2), where $(\alpha, \tau) \in \mathbb{R} \times \mathbb{R}$. $\varphi(x)$ and $\Phi(x)$ are the PDF and cumulative distribution function (CDF) of the standard Gaussian distribution calculated at x. It reduces to the PDF of a standard SN random when $\tau = 0$.

$$\varphi(x;\alpha,\tau) = \varphi(x)\frac{\Phi(\tau\sqrt{1+\alpha^2}+\alpha x)}{\Phi(\tau)},\quad x \in \mathbb{R} \tag{2}$$

Generally for any variable of type $Y = \xi + \omega Z$, if Z has a density function of (2), the CDF of Y is the integral from $-\infty$ to $\frac{y-\xi}{\omega}$. The PDF of Y can be obtained by the derivative of CDF, as is shown in (3), briefly $ESN(\xi,\omega,\alpha,\tau)$. Given the dataset from SPICE simulations, (ξ,ω,α,τ) can be calculated through the log-likelihood function [17]. Nevertheless, it cannot accurately estimate the $+/-3\sigma$ delay because the distribution does not accurately follow the ESN distribution.

$$\frac{1}{\omega}\varphi\left(\frac{x-\xi}{\omega}\right)\frac{\Phi(\tau\sqrt{1+\alpha^2}+\alpha\frac{x-\xi}{\omega})}{\Phi(\tau)}. \tag{3}$$

B. Exponential Process Variation Effects

Defined by manufacturing foundry, a MOSFET model contains lots of process parameters ($process_i$) in the form of (4). Given a cell netlist, parameters of each MOSFET are defined and determine the constant $process_{i,0}$. Each process parameter is affected by a global variation ($\delta pv_{i,g}$) and a local variation ($\delta pv_{i,l}$), representing die-to-die and with-in-die [6], respectively. Each variation is a Gaussian random variable, so the $process_i$ of the linear combination also follows the Gaussian distribution. However, these process parameters do not linearly affect the cell delay. In the analytical-based cell delay models [4], part of variations (e.g., X_L) linearly affect the delay while part of them have an exponential impact (e.g., V_{th}). A detailed analysis of each process parameter is provided in [22] using canonical correlation analysis.

$$process_i = process_{i,0} + \delta pv_{i,g} + \delta pv_{i,l} \tag{4}$$

Considering that the process variation effect of the exponential term is dominants, we give a cell delay model which converts the delay to a logarithmic form. The logarithmic operation quantifies the exponential process variation effect and the result follows an ESN distribution to fit the skewness and kurtosis. Given the random ESN variable Y followed by (3), the cell delay distribution (T_d) can be represented as $\log(T_d) = Y, Y \sim ESN(\xi,\omega,\alpha,\tau)$. The distribution function of T_d can be deduced through (6). Then, the PDF of T_d can be obtained by the derivative of (5), and it equals to (6), briefly $LESN(\xi,\omega,\alpha,\tau)$. The parameters of the LESN distribution can be estimated using $\log(T_d)$ and log-likelihood function of ESN in (7), where v represents $\tau\sqrt{1+\alpha^2}+\alpha(x-\xi)/\omega$.

$$F(T_d) = P(\exp(Y) \le T_d) = P(Y \le \log(T_d))$$
$$= \int_{-\infty}^{\log(T_d)} \frac{1}{\omega}\varphi\left(\frac{x-\xi}{\omega}\right)\frac{\Phi(\tau\sqrt{1+\alpha^2}+\alpha\frac{x-\xi}{\omega})}{\Phi(\tau)}\,dx \tag{5}$$

$$\frac{1}{\omega x}\varphi\left(\frac{\log(x)-\xi}{\omega}\right)\frac{\Phi(\tau\sqrt{1+\alpha^2}+\alpha\frac{\log(x)-\xi}{\omega})}{\Phi(\tau)} \tag{6}$$

$$\log(\Phi(v)) - \log(\Phi(\tau)) - \log(\sqrt{2\pi}\omega) - \frac{1}{2}\left(\frac{x-\xi}{\omega}\right)^2 \tag{7}$$

Fig. 4 shows the fitting results using LSN, Burr, ESN, and LESN distributions, compared to the INV delay distribution from SPICE simulation. Each of these models is constructed using corresponding log-likelihood functions. As the distribution has a relatively heavy right tail in low voltage regions, the LESN-based fitting model can match the curve shape more precisely, either for the heavy right tail or for the light

Authorized licensed use limited to: Chinese University of Hong Kong. Downloaded on November 22,2026 at 12:59:40 UTC from IEEE Xplore. Restrictions apply.

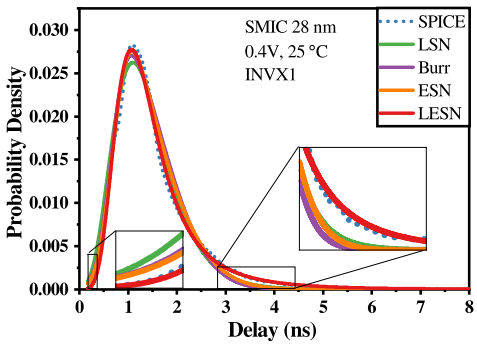

Fig. 4. Comparison of the fitting result based on LSN, Burr, ESN, and LESN.

TABLE I
ERRORS OF ESTIMATING $+/-3\sigma$ DELAY USING LSN, BURR, AND LESN DISTRIBUTIONS (FO4, 25°C)

Voltage	Cell Name	LSN [6]		Burr [8]		LESN	
		-3σ	+3σ	-3σ	+3σ	-3σ	+3σ
0.4V	INV	3.66	5.31	16.10	61.96	0.97	2.09
	NAND2	4.39	4.94	21.25	56.89	2.71	2.96
	NOR2	5.04	7.13	21.61	53.66	3.57	4.81
0.7V	INV	0.93	1.99	4.79	6.45	0.68	1.38
	NAND2	0.71	1.96	6.52	9.66	0.64	1.61
	NOR2	0.74	5.32	6.51	9.81	0.83	1.77
1.1V	INV	0.76	0.57	2.28	3.01	0.33	0.89
	NAND2	0.61	0.66	4.58	3.13	0.99	0.48
	NOR2	0.79	0.32	4.42	4.38	0.74	0.34
Average Error		1.96	3.13	9.79	23.22	1.27	1.82

* Input transition time of the cell is constant (10ps)

left tail. At normal voltage (1.1V), the delay distribution has little skewness and same length of left and right tails, the parameters α and τ are reduced to zero. The LESN distribution will turn to LN distribution at normal voltage, which is verified to be highly accurate in previous studies [2], [6]. Hence, the LESN model is suitable for wide voltage ranges.

When the load capacitance is increased, the mean and standard deviation of the delay distribution is linearly affected as the capacitance has a linear effect on the cell delay, which is modeled in several analytical delay models. Given a load capacitance C_L, the parameters of the LESN distribution can be obtained in (8). The coefficient vectors A and B are fitted by using the estimated LESN parameters with different fan-out constraints (from FO1 to FO8). As the cell delay is linearly affected, the skewness and kurtosis will be little changed and the coefficient of α and τ in A and B is near to zero.

$$[\xi, \omega, \alpha, \tau] = A * C_L + B. \tag{8}$$

V. RESULTS

A. Experimental Setup

The delay distributions of standard cells (INV, NAND2, and NOR2) are modeled and verified using SMIC 28 nm PDK. The supply voltage is set to be 0.4V as sub-threshold region, 0.7V as near-threshold region, and 1.1V as normal threshold region. The fan-out constraints of each cell are set to be FO1, FO2, FO4, and FO8. The accuracy of cell delay models are verified by comparing to the data obtained through SPICE simulations with 10k Monte Carlo samples under global and local variations.

B. Delay Distribution Accuracy

As the complicated supply voltage effect on the drain current [4], the proposed delay model is built at a specific supply voltage and needs to be rebuilt if the voltage changed. However, the model still has high accuracies on estimating the mean and standard deviation of the delay distribution (the relative errors are less than 0.1% and 1%, respectively). Fig. 5 shows the errors of estimating the skewness and kurtosis using LSN and LESN distributions, built under the FO1 constraint at 0.4V and 0.7V. The average errors of the skewness and kurtosis are less than 2% both at 0.4V and 0.7V. The results at 1.1V are not given because the skewness is always near 0 while the kurtosis is always near 3. Due to the introduction of logarithmic operation, the two moments cannot be deduced theoretically either in the LSN distribution or in the LESN distribution. Similar to the method given in [6], they are estimated by sampling 10k times from the CDF of each model.

To cover different fan-out constraints, the parameters in the LESN distribution are modeled using (8) and are verified at 0.4V and 0.7V separately. Fig. 6 shows the errors of the mean (μ), standard deviation (σ), skewness (γ), and kurtosis (k) under the load constraints of FO1, FO2, FO4, and FO8, respectively. The errors of the mean and standard deviation are less than 0.1% and 1%, both at 0.4V and 0.7V. As the skewness and kurtosis are very small at 0.7V, the relative errors seem larger (e.g., 0.1 v.s. 0.12). Despite that, the model can still match the shape of the curve.

The 3σ delay is defined as an important metric of the delay distribution to represent the worst-case and the best-case of the standard cell. The $+3\sigma$ delay is the value of the X-axis when the Y-axis of the CDF is 99.86%. Similarly, the -3σ delay is the point when the Y-axis is 0.14%. Table I shows the errors of estimated $+/-3\sigma$ delay using LSN, Burr, and LESN models, tested under the constraint of FO4. Obviously, Burr-based model cannot be used for estimating the $+3\sigma$ delay in the sub-threshold voltage region. As the skewness and kurtosis at 0.7V is relatively small, the average error of LSN-based delay model is less than 5%. However, the moments get larger at 0.4V, which causes the average error of the LSN-based model much higher. On the contrary, the error of the LESN-based model is always less than 2% for each cell at 0.7V and 1.1V. In the sub-threshold region, the peak of the NOR2 delay distribution tested by the second input pin becomes extremely sharp, and the kurtosis will be higher than 100. Even so, the error for estimating the $+3\sigma$ delay is still less than 5%. On average, the error for the -3σ delay and $+3\sigma$ delay estimations are about 1.27% and 1.82%, respectively.

VI. CONCLUSION

In this brief, an LESN-based model is proposed for accurately estimating the cell delay distribution from the sub-threshold voltage region to the normal voltage region. The shape of the cell delay distribution is modeled by matching

Authorized licensed use limited to: Chinese University of Hong Kong. Downloaded on November 22,2026 at 12:59:40 UTC from IEEE Xplore. Restrictions apply.

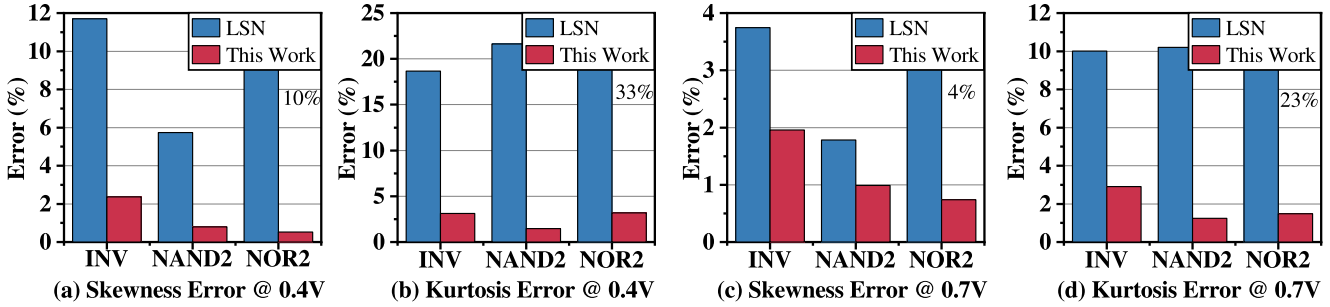

Fig. 5. Errors of estimated skewness and Kurtosis (errors are calculated at 25°C through: $Error = \frac{abs(sim-model)}{sim} * 100\%$).

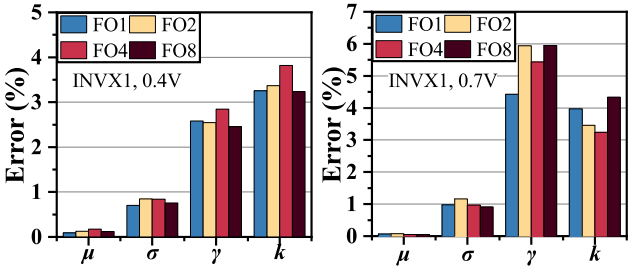

Fig. 6. Errors of LESN model with different fanout constraints.

the mean, standard deviation, skewness, and kurtosis at the same time. Considering the load capacitance effect, a linear model is proposed to get the four parameters of the LESN distribution at different fan-out constraints. The delay model has a high precision on estimating the $+/-3\sigma$ delay either in subthreshold voltage region or in near-threshold voltage region. The errors for estimating the moments are all less than 5% and the average errors for $+/-3\sigma$ are both less than 2%. In our future work, more effects will be modeled combined with the LESN model, such as the input effect of the cell, including the input transition time and the multiple-input switching behavior.

REFERENCES

[1] D. Blaauw, K. Chopra, A. Srivastava, and L. Scheffer, "Statistical timing analysis: From basic principles to state of the art," *IEEE Trans. Comput.-Aided Design Integr. Circuits Syst.*, vol. 27, no. 4, pp. 589–607, Apr. 2008.

[2] S. Keller, D. M. Harris, and A. J. Martin, "A compact transregional model for digital CMOS circuits operating near threshold," *IEEE Trans. Very Large Scale Integr. (VLSI) Syst.*, vol. 22, no. 10, pp. 2041–2053, Oct. 2014.

[3] F. Frustaci, P. Corsonello, and S. Perri, "Analytical delay model considering variability effects in subthreshold domain," *IEEE Trans. Circuits Syst. II, Exp. Briefs*, vol. 59, no. 3, pp. 168–172, Mar. 2012.

[4] P. Cao, Z. Liu, J. Guo, and J. Wu, "An analytical gate delay model in near/subthreshold domain considering process variation," *IEEE Access*, vol. 7, pp. 171515–171524, 2019.

[5] D. Sinha *et al.*, "Statistical timing analysis considering multiple-input switching," in *Proc. 57th ACM/IEEE Des. Autom. Conf. (DAC)*, San Francisco, CA, USA, 2020, pp. 1–6.

[6] H. A. Balef, M. Kamal, A. Afzali-Kusha, and M. Pedram, "All-region statistical model for delay variation based on log-skew-normal distribution," *IEEE Trans. Comput.-Aided Design Integr. Circuits Syst.*, vol. 35, no. 9, pp. 1503–1508, Sep. 2016.

[7] C. Visweswariah *et al.*, "First-order incremental block-based statistical timing analysis," *IEEE Trans. Comput.-Aided Design Integr. Circuits Syst.*, vol. 25, no. 10, pp. 2170–2180, Oct. 2006.

[8] A. Moshrefi, H. Aghababa, and O. Shoaei, "Statistical estimation of delay in nano-scale CMOS circuits using burr distribution," *Microelectron. J.*, vol. 79, pp. 30–37, Sep. 2018.

[9] K. Chopra, B. Zhai, D. Blaauw, and D. Sylvester, "A new statistical max operation for propagating skewness in statistical timing analysis," in *Proc. IEEE/ACM Int. Conf. Comput.-Aided Design*, San Jose, CA, USA, 2006, pp. 237–243.

[10] F. J. Cazorla, L. Kosmidis, E. Mezzetti, C. Hernandez, J. Abella, and T. Vardanega, "Probabilistic worst-case timing analysis: Taxonomy and comprehensive survey," *ACM Comput. Surv.*, vol. 52, no. 1, pp. 1–35, 2019.

[11] T.-J. Lee, T.-Y. Tsai, W. Lin, U.-F. Chio, and C.-C. Wang, "A slew rate variation compensated 2× VDD I/O buffer using deterministic P/N-PVT variation detection method," *IEEE Trans. Circuits Syst. II, Exp. Briefs*, vol. 66, no. 1, pp. 116–120, Jan. 2019.

[12] Z. Feng, P. Li, and Y. Zhan, "Fast second-order statistical static timing analysis using parameter dimension reduction," in *Proc. 44th ACM/IEEE Des. Autom. Conf.*, 2007, pp. 244–249.

[13] S. Ramprasath, M. Vijaykumar, and V. Vasudevan, "A skew-normal canonical model for statistical static timing analysis," *IEEE Trans. Very Large Scale Integr. (VLSI) Syst.*, vol. 24, no. 6, pp. 2359–2368, Jun. 2016.

[14] T. Liu, C.-C. Chen, and L. Milor, "Accurate standard cell characterization and statistical timing analysis using multivariate adaptive regression splines," in *Proc. 16th Int. Symp. Qual. Electron. Des.*, Santa Clara, CA, USA, 2015, pp. 272–279.

[15] W. Fu, L. Jin, M. Ling, Y. Zheng, and L. Shi, "A cross-layer power and timing evaluation method for wide voltage scaling," in *Proc. 57th ACM/IEEE Des. Autom. Conf. (DAC)*, San Francisco, CA, USA, 2020, pp. 1–6.

[16] W. Fu, L. Jin, M. Ling, Y. Zheng, and L. Shi, "VASTA: A wide voltage statistical timing analysis tool based on variation-aware cell delay models," *IEEE Access*, vol. 8, pp. 197194–197202, 2020.

[17] P. H. Westfall, "Kurtosis as peakedness, 1905–2014. R.I.P." *Amer. Stat.*, vol. 68, no. 3, pp. 191–195, 2014.

[18] P. Cao, Z. Liu, B. Xu, and J. Guo, "A statistical timing model for CMOS inverter in near-threshold region considering input transition time," in *Proc. 26th IEEE Int. Conf. Electron. Circuits Syst. (ICECS)*, Genoa, Italy, 2019, pp. 586–589.

[19] P. Pandey, P. Basu, K. Chakraborty, and S. Roy, "GreenTPU: Improving timing error resilience of a near-threshold tensor processing unit," in *Proc. 56th ACM/IEEE Des. Autom. Conf. (DAC)*, Las Vegas, NV, USA, 2019, pp. 1–6.

[20] A. C. Ranasinghe and S. H. Gerez, "MEPNTC: A standard-cell library design scheme extending the minimum-energy-point operation of near-V_{th} computing," in *Proc. IEEE 38th Int. Conf. Comput. Des. (ICCD)*, Hartford, CT, USA, 2020, pp. 96–104.

[21] A. Azzalini, *The Skew-Normal and Related Families*, vol. 3. Cambridge, U.K.: Cambridge Univ. Press, 2013.

[22] H. G. Mohammadi, P.-E. Gaillardon, and G. De Micheli, "Efficient statistical parameter selection for nonlinear modeling of process/performance variation," *IEEE Trans. Comput.-Aided Design Integr. Circuits Syst.*, vol. 35, no. 12, pp. 1995–2007, Mar. 2016.

Authorized licensed use limited to: Chinese University of Hong Kong. Downloaded on November 22,2026 at 12:59:40 UTC from IEEE Xplore. Restrictions apply.